Cell Transplantation
2019, Vol. 28(6) 756–766

DOI: 10.1177/0963689718822809
journals.sagepub.com/home/cll
SAGE

Administration of rCTRP9 Attenuates Neuronal Apoptosis Through AdipoR1/PI3K/Akt Signaling Pathway after ICH in Mice

Lianhua Zhao[1,2], John H. Zhang[2], Prativa Sherchan[2], Paul R. Krafft[3], Wei Zhao[1], Sa Wang[4], Shengpan Chen[2,5], Zaiyu Guo[1], and Jiping Tang[2]

Abstract

Targeting neuronal apoptosis after intracerebral hemorrhage (ICH) may be an important therapeutic strategy for ICH patients. Emerging evidence indicates that C1q/TNF-Related Protein 9 (CTRP9), a newly discovered adiponectin receptor agonist, exerts neuroprotection in cerebrovascular disease. The aim of this study was to investigate the anti-apoptotic role of CTRP9 after experimental ICH and to explore the underlying molecular mechanisms. ICH was induced in mice via intrastriatal injection of bacterial collagenase. Recombinant CTRP9 (rCTRP9) was administrated intranasally at 1 h after ICH. To elucidate the underlying mechanisms, adiponectin receptor1 small interfering ribonucleic acid (AdipoR1 siRNA) and selective PI3 K inhibitor LY294002 were administered prior to rCTRP9 treatment. Western blots, neurofunctional assessments, immunofluorescence staining, and Fluoro-Jade C (FJC) staining experiments were performed. Administration of rCTRP9 significantly improved both short- and long-term neurofunctional behavior after ICH. RCTRP9 treatment significantly increased the expression of AdipoR1, PI3 K, p-Akt, and Bcl-2, while at the same time was found to decrease the expression of Bax in the brain, which was reversed by inhibition of AdipoR1 and PI3 K. The neuroprotective effect of rCTRP9 after ICH was mediated by attenuation of neuronal apoptosis via the AdipoR1/PI3K/Akt signaling pathway; therefore, rCTRP9 should be further evaluated as a potential therapeutic agent for ICH patients.

Keywords

intracerebral hemorrhage, adiponectin receptor 1, C1q/TNF-related protein 9, neuronal apoptosis, PI3K/Akt signaling

Introduction

Intracerebral hemorrhage (ICH) is a stroke subtype with a high mortality and morbidity rate that accounts for 10–15% of all strokes worldwide[1–3]. Despite its devastating socio-economic burden on individuals and society, ICH remains an unresolved medical problem with little improvement in patient outcomes over the past 20 years[4]. Regarding the pathophysiology of ICH, it is generally accepted that the intraparenchymal hematoma compressing the surrounding brain tissue is considered to elicit the primary brain injury; then red blood cell debris and other clot components lead to secondary brain injury (SBI), which involves a series of molecular processes including inflammatory responses, activation of apoptosis cascades, ischemia, blood–brain barrier disruption, and brain edema formation. Apoptosis is the main form of cell death within the brain region surrounding the intracerebral hematoma[5,6]. Furthermore, it has been

[1] Department of Neurology, Tianjin TEDA Hospital, Tianjin, China
[2] Department of Physiology and Pharmacology, Loma Linda University, Loma Linda, CA, USA
[3] Department of Neurological Surgery and Brain Repair, Morsani College of Medicine, University of South Florida, Tampa, FL, USA
[4] Department of Neurology, Affilicated Wenling Hospital of Wenzhou Medical University, Wenling, Zhejiang, China
[5] Department of Neurosurgery, Affiliated Haikou Hospital, Xiangya School of Medicine, Central South University, Haikou, China

Submitted: October 15, 2018. Revised: December 3, 2018. Accepted: December 11, 2018.

Corresponding Authors:
Jiping Tang, MD, Department of Physiology and Pharmacology, Loma Linda University, 11041 Campus St, Loma Linda, CA 92354, USA; Zaiyu Guo, MD, PhD, Department of Neurosurgery, Tianjin TEDA Hospital, No.65 The 3th Avenue, Tianjin TEDA, China.
Emails: jtang@llu.edu; guozai_yu@163.com

shown that the extent of neuronal apoptosis is closely related to impaired neurological functions[7,8]. Therefore, inhibiting neuronal apoptosis after ICH may alleviate neurological deficits and improve overall patient outcomes.

Adiponectin (APN) is an adipose-derived secretory serum protein that has been shown to alter multiple functions in the peripheral and central nervous systems[9–11]. However, APN knock-out mice exhibit highly variable phenotypes[12]. Because APN has a C-terminal globular domain with sequence homology to the immune complement protein C1q, it belongs to the larger family of C1q proteins[13]. C1q/TNF-related proteins (CTRPs) have similar structural and biochemical properties as APN[14–16]. Of all identified CTRPs, CTRP9 shares the highest degree of sequence identity (54%) with APN at the presumed functional globular domain[15].

APN exerts its physiological effects by binding to and thereby activating its specific receptors. Currently two APN receptors, AdipoR1 and AdipoR2, have been identified. AdipoR1 is widely expressed in the central nervous system (CNS), especially on neurons[17]. It has been reported that AdipoR1 agonists participate in neuroprotective actions against ischemic stroke, particularly by reducing neuronal apoptosis[18]. Two recent studies suggest that the anti-apoptotic effects of AdipoR1 agonists are mediated via the phosphatidylinositol 3-kinase (PI3 K)/ protein kinase B (Akt) signaling pathway[19,20]. It has been shown that CTRP9 exerts a high affinity to AdipoR1[21], and emerging evidence suggests that CTRP9 has the potential to carry out neuroprotective functions on diverse CNS disease[22]. However, the anti-apoptotic effects of CTRP9 following ICH have not yet been illustrated.

The present study aimed to assess the effects of CTRP9 on neurofunctional outcomes and neuronal apoptosis in mice subjected to experimental ICH. The mechanisms of the observed effects were then explored using AdipoR1 siRNA and PI3 K inhibitor, LY294002.

Materials and Methods

Animals

A total of 144 male CD1 mice (8 weeks old, weight 30–40 g; Charles River, Wilmington, MA, USA) were housed in a temperature and humidity-controlled room with a 12-hour light/dark cycle and free access to food and water. All animals were acclimated to the environment for a minimum of 3 days before being subjected to ICH induction or sham surgery. The experimental protocols and procedures for this study were approved by the Institutional Animal Care and Use Committee (IACUC) at Loma Linda University (IACUC No. 8160049) and were in compliance with the National Institutes of Health's Guide for the Care and Use of Laboratory Animals.

ICH Model and Study Design

Experimental ICH was induced in mice by intrastriatal injection of bacterial collagenase, as previously reported[23]. Briefly, mice were anesthetized with a mixture of ketamine (100 mg/kg) and xylazine (10 mg/kg) (2:1, intraperitoneal injection) and positioned prone in a stereotaxic head frame (Kopf Instruments, Tujunga, CA, USA). A 1-mm cranial burr hole was drilled, and a 26-gauge needle on a 10-μl Hamilton syringe was inserted stereotactically into the right striatum (coordinates 0.2 mm posterior, 2.2 mm lateral to the bregma, and 3.5 mm below the dura). Bacterial collagenase type VII-S (0.075 units) (Sigma-Aldrich, St. Louis, MO, USA) dissolved in 0.5 μl sterile phosphate-buffered saline (PBS) was infused into the brain at a rate of 0.167 μl/min with an infusion pump (Stoelting, Harvard Apparatus, Holliston, MA, USA). The needle was left in place for an additional 5 min after the injection to prevent possible leakage of the collagenase solution before being withdrawn slowly at a rate of 1 mm/min. The cranial burr hole was sealed with bone wax, the scalp was sutured, and 0.4 ml of normal saline was injected subcutaneously to avoid postsurgical dehydration. Mice were allowed to recover fully under close observation. The sham operation was performed following the same protocol but involved needle insertion only.

All mice were randomly assigned to the following four separate experiments as shown in the timeline of the experimental design (Additional file 1: Fig. S1). Experimental groups, animal numbers, and mortality rates of this current study are summarized in the supplemental material (Additional file 2: Table S1).

Experiment 1. To determine the time course of endogenous AdipoR1 and CTRP9 expression in the brain of mice subjected to ICH, n=36 mice were divided into six groups (n=6/group) including sham as well as ICH after 3, 6, 12, 24, and 72 h. Two additional mice were used for double immunohistochemistry staining of AdipoR1 combined with specific markers for neurons, astrocytes, and microglia at 24 h after ICH.

Experiment 2. To evaluate the short-term neurofunctional deficits and the extent of neuronal apoptosis, n=27 mice were randomly divided into three groups (n=9/group): sham, ICH+vehicle (PBS), ICH+rCTRP9 (0.1 μg/g). Recombinant CTRP9 (rCTRP9) was administered intranasally at 1 h post-ICH. Neurofunctional tests and Fluoro-Jade C (FJC) staining were conducted at 24 h post-ICH.

Experiment 3. To assess long-term neurofunctional deficits, n=24 mice were divided into three groups (n=8/group): sham, ICH+vehicle (PBS), ICH+rCTRP9 (0.1 μg/g). The foot-fault test and rotarod test were performed on days 7, 14, and 21 post-ICH, and the Morris water maze test was conducted on days 21–25 post-ICH.

Experiment 4. To verify the anti-apoptotic mechanism of rCTRP9, n=42 mice were divided into seven groups (n=6/group): sham, ICH+vehicle (PBS), ICH+rCTRP9 (0.1 μg/g), ICH+rCTRP9+AdipoR1 siRNA, ICH+rCTRP9+Scramble

siRNA (Scr siRNA), ICH+rCTRP9+LY294002 (specific PI3 K inhibitor), ICH+rCTRP9+DMSO (5 µl of 5% dimethyl sulfoxide in PBS). LY294002 and DMSO were delivered intracerebroventricularly 30 min before ICH[24] and scrambled siRNA and AdipoR1 siRNA were injected intracerebroventricularly 48 h before ICH[25]. Neurofunctional testing and western blot were performed at 24 h post-ICH.

Western Blot Analysis

Western blot was performed as previously described[26]. Briefly, mice were transcardially perfused with ice-cold PBS under deep anesthesia, and brains were removed and separated into two hemispheres at 24 h after ICH induction or sham surgeries. The ipsilateral/right brain hemispheres were homogenized in RIPA lysis buffer (Santa Cruz Biotechnology, Santa Cruz, CA, USA) and centrifuged at 4°C for 30 min at 14,000 *g*. The supernatant was collected, and the protein concentration was determined using a detergent compatible assay (DC protein assay, Bio-Rad Laboratories, CA, USA). Equal amounts of protein were loaded on an SDS-PAGE gel and run using electrophoresis and then transferred to a nitrocellulose membrane. The membrane was blocked and incubated at 4°C overnight with the following primary antibodies targeting: CTRP9 (1:500, NBP2-46834, Novus, Centennial, CO, USA), AdipoR1 (1:1000, ab126611, Abcam, Cambridge MA, USA), PI3 K (1:1000, ab182651, Abcam), p-Akt (1:1000, #9271, Cell Signaling Technology, Boston (CST), MA, USA), Akt (1:2000, #9271, CST), Bcl-2 (1:1000, #2764, CST), Bax (1:500, NBP1-28566, Novus Biologicals) and actin (1:4000, Santa Cruz Biotechnology, Dallas, TX, USA). Appropriate secondary antibodies (1:3000, Santa Cruz Biotechnology; 1:5000, Abcam) were selected to incubate with the membrane for 2 h at room temperature. The bands were probed with an ECL Plus chemiluminescence regent kit (Amersham Biosciences, Arlington Heights, PA, USA) and visualized with the image system (Bio-Rad, Versa Doc, model 4000). Relative density of the protein immunoblot images were analyzed by ImageJ software (ImageJ 1.4, National Institutes of Health (NIH), Bethesda, MD, USA).

Immunofluorescence Staining

The brain samples used for immunohistochemistry staining were prepared according to a previously described protocol[27]. Briefly, animals were deeply anesthetized at 24 h after ICH and transcardially perfused with 100 ml ice-cold PBS followed by 60 ml of 10% paraformaldehyde. The whole brain was collected and fixed in 10% paraformaldehyde for 24 h and dehydrated in a 30% sucrose solution for 3 days. After being kept frozen at –80°C, brains were cut into 8 µm-thick coronal sections on a cryostat (LM3050 S; Leica Microsystems, Bannockburn, Germany). Immunofluorescence staining was conducted as previously described[28]. Briefly, brain samples were incubated overnight at 4°C with the primary antibodies including anti-Iba-1 (1:200, ab178847, Abcam), anti-NeuN (1:200, ab177487, Abcam) and anti-GFAP (1:200, ab16997, Abcam), and anti-AdipoR1 (1:200, ab126611, Abcam). The corresponding secondary antibodies (1:500, Jackson Immunoresearch, West Grove, PA, USA) were added to the brain sections and allowed to incubate at room temperature for 2 h. The sections were visualized and photographed by using a fluorescence microscope (Leica Microsystems).

Short-Term Neurofunctional Assessments

Short-term neurofunctional behavior was assessed with the modified Garcia score, forelimb placement test, and corner turn test involving an independent researcher blinded to the experimental groups. All tests were performed at 24 h after ICH induction or sham surgery, as previously described[29,30]. The Garcia score includes seven individual tests that evaluate spontaneous activity, vibrissae proprioception, axial sensation, symmetry of limb movement, lateral turning, forelimb walking, and climbing. Each subtest was given a score ranging from 0 to 3, with a composite maximum score of 21 (no neurological deficits). The forelimb placement test was used to assess the animals' responsiveness to vibrissae stimulation, and results were expressed as a percentage of the number of successful left forepaw placements out of 10 stimulations, normalized to the mean of sham performance. For the corner turn test, animals were allowed to advance into a 30° corner and exit by turning either to the left or right. Choice of turning was recorded for a total of 10 trials, and a score was calculated as number of left turns/all trials × 100.

Fluoro-Jade C Staining

Degenerating neurons were evaluated by FJC staining as previously described utilizing a modified FJC ready-to-dilute staining kit (Biosensis, USA) according to the manufacturer's instructions[31,32]. Briefly, FJC-positive neurons were counted in six sections per brain at ×200 magnification by an independent observer. Quantified analysis was performed with Image J software (Image J 1.4, NIH, Bethesda, MD, USA). The data were presented as the average number of FJC-positive neurons in the fields (cells/mm^2).

Drug Administration

Recombinant CTRP9 (rCTRP9) (cat# H00338872-P01, Novus Biologicals) dissolved in PBS was administered intranasally at 1 h post-ICH as previously reported[27]. A total volume of 20 µl of rCTRP9 solution was administered intranasally. Mice under anesthesia were placed in a supine position and rCTRP9 solution was administered in drops (5 µl/drop) every 2 min, alternating between the left and right nares, over a period of approximately 20 min. The ICH+vehicle group was given an equal volume of PBS intranasally. The method for drug administration was the same for short- and long-term experiments.

Long-Term Neurofunctional Assessments

To evaluate the long-term neurofunctional outcomes after ICH, the foot-fault and rotarod tests were performed within the first, second, and third week post-ICH as previously described[33]. These tests specifically evaluate the rodents' sensorimotor function, coordination, and balance. Water maze tests were performed on days 21 to 25 post-ICH to evaluate memory and spatial learning as previously described[34].

Intracerebroventricular Injection

Intracerebroventricular administration was performed as previously described[35]. AdipoR1 siRNA (cat# 4390771) and Scramble siRNA (scr siRNA) (cat# 4390843, Life Technologies, Carlsbad, CA, USA) were prepared at 500 pmol in RNAse-free suspension buffer and were infused (5 μl of the siRNAs) 48 h before ICH modeling in ICH+rCTRP9+AdipoR1 siRNA and ICH+rCTRP9+Scr siRNA mice, respectively. LY294002 (Selleck Chemicals, Houston, TX, USA) was prepared at 50 mmol/l in PBS (contains 25% DMSO), and 5 μl of the DMSO and LY294002 were infused 30 min before ICH induction in ICH+rCTRP9+LY294002 and ICH+rCTRP9+DMSO mice, respectively. The 26-gauge needle of a 10-μl Hamilton syringe was inserted into the left lateral ventricle through a cranial burr hole at the following coordinates relative to bregma: 0.3 mm posterior, 1.0 mm lateral, and 2.3 mm below the dura. A micro-infusion pump was used for the intracerebroventricular administrations at a rate of 0.667 μl/min. The needle was left in place for an additional 5 min after the end of infusion before being slowly withdrawn over 3 min. The burr hole was sealed with bone wax.

Statistical Analysis

All data were expressed as the mean and standard deviation (mean ± SD). Statistical analysis was performed with Graph Pad Prism (Graph Pad Software Inc., San Diego, CA, USA). Data were analyzed by one-way analysis of variance (ANOVA) followed by multiple comparisons between groups using Tukey's post-hoc test. A P-value of less than 0.05 was considered statistically significant.

Results

Animal Mortality and Exclusion

None of the sham animals died prior to euthanasia. The total animal mortality rate in this study was 11.3% (13/115). The mortality rate was not significantly different between the experimental groups (Additional file 2: Table S1).

The Endogenous Expressions Time Course of AdipoR1 and CTRP9 after ICH

Western blot was performed to assess the protein expression of AdipoR1 and CTRP9 in the ipsilateral/right cerebral hemispheres of sham animals or at 3, 6, 12, 24, and 72 h after ICH induction. The endogenous expressions of AdipoR1 and CTRP9 continuously increased after surgery, reached a peak at 24 h, and then decreased again at 72 h after ICH induction ($p<0.05$ compared with sham, Fig. 1A, B). Double immunofluorescence staining was performed to detect the localization of AdipoR1 on neurons (NeuN), microglia/macrophages (Iba-1), and astrocytes (GFAP) at 24 h after ICH. AdipoR1 was mainly expressed on neurons and astrocytes after ICH (Fig. 1C).

rCTRP9 Ameliorated Short-Term Neurofunctional Deficits after ICH

ICH induction significantly reduced the composite modified Garcia score, as well as performances of the forelimb placement and corner turn test at 24 h after surgery when compared with sham animals. The neurofunctional impairments were significantly ameliorated by administration of rCTRP9 (0.1 μg/g) as seen in the ICH+rCTRP9 group, ($p<0.05$ compared with the vehicle group, Fig. 2A–C).

rCTRP9 Attenuated Neuronal Apoptosis after ICH

FJC was used to evaluate the severity of neuronal degeneration and apoptosis in the ipsilateral hemisphere at 24 h after ICH (Fig. 3B). ICH induction resulted in a significantly increased number of FJC-positive cells (ICH+vehicle) when compared with sham animals ($p<0.05$); however, rCTRP9 treatment (0.1 μg/g) significantly reduced the number of apoptotic cells as demonstrated in the ICH+rCTRP9 group ($p<0.05$ compared with ICH+vehicle, Fig. 3A and C).

rCTRP9 Improved Long-Term Neurofunctional Outcomes after ICH

At the first, second, and third week after surgery, mice randomized to the ICH+vehicle group demonstrated significantly more foot faults of the left forelimb as well as shorter falling latencies than those animals randomized to the sham group ($p<0.05$, Fig. 4A, B). However, animals in the ICH+rCTRP9 group demonstrated significantly fewer missteps with the left forelimb as well as longer walking periods on the rotarod before falling when compared with the vehicle group ($p<0.05$, Fig. 4A, B).

During Morris water maze testing, the swim distance and escape latency measured for vehicle animals to find a platform within a pool of water were found significantly increased when compared with the sham group ($p<0.05$, Fig. 4C, D). However, a significantly shorter swim distance and escape latency was observed in the ICH+rCTRP9 group on days 3 to 5 of testing ($p<0.05$ compared with ICH+vehicle, Fig. 4C, D).

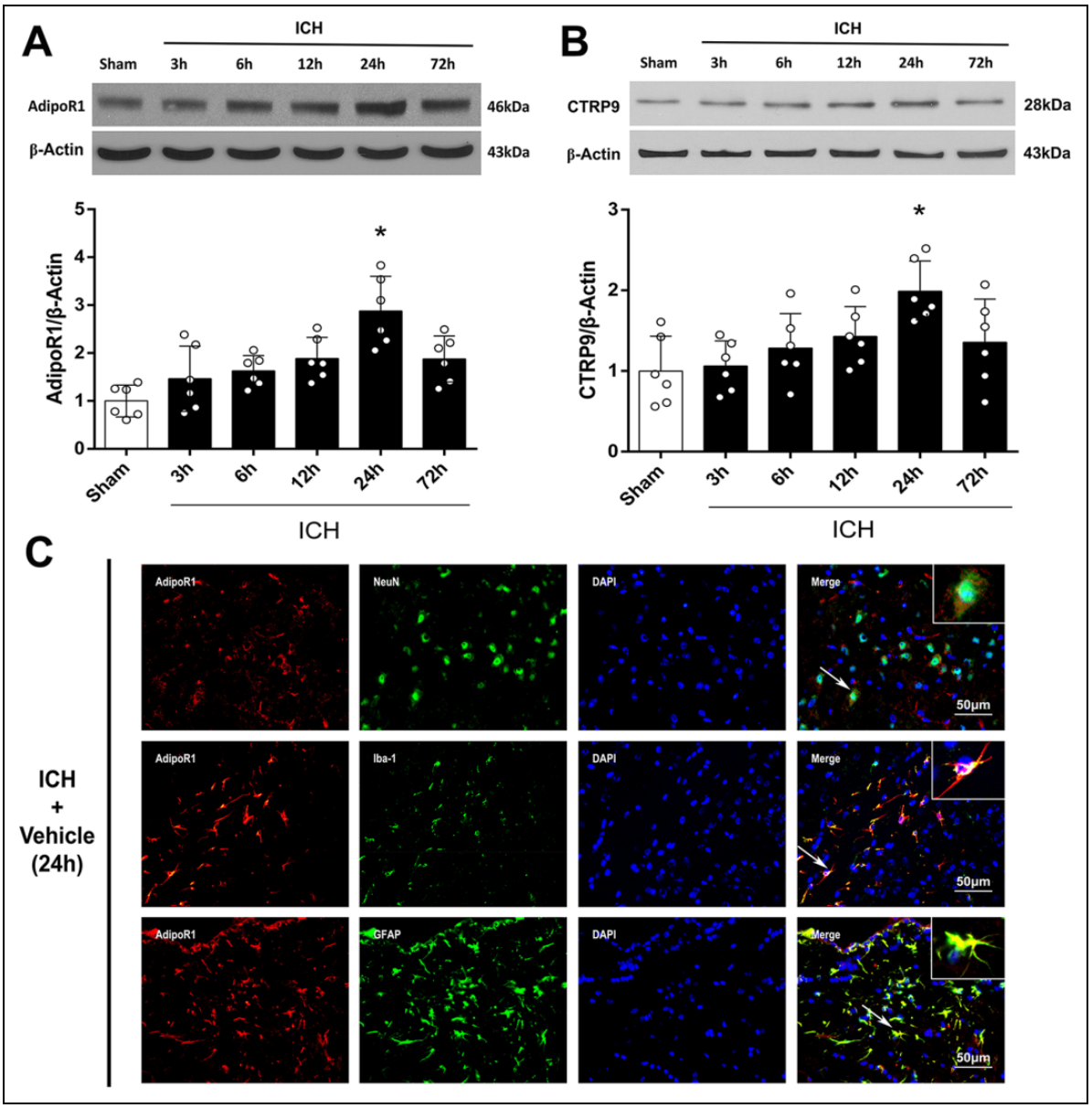

Figure 1. Expression of adiponectin receptor 1 (AdipoR1) and C1q/TNF-related protein 9 (CTRP9) at 24 h after intracerebral hemorrhage (ICH). (A) Representative western blot images and quantitative analyses of AdipoR1 time course after ICH. (B) Representative western blot images and quantitative analyses of CTRP9 time course after ICH. Values are expressed as mean ± SD. *p<0.05 vs. sham group. N=6. (C) Double immunofluorescence staining for AdipoR1 (red) in neurons (NeuN, green), microglia (Iba-1, green), and astrocytes (GFAP, green) in right basal cortex 24 h after ICH. Scale bar=50μm. N=2. DAPI, 4',6-diamidino-2-phenylindole; Iba-1, NeuN, neuronal nuclear; ionized calcium binding adaptor molecule-1; GFAP, glial fibrillary acidic protein.

AdipoR1 siRNA and PI3 K Inhibitor Reversed the Neurofunctional Improvements Seen with rCTRP9 Therapy

Administration of rCTRP9 resulted in improved neurofunctional performances after ICH, which was assessed via neurofunctional tests including the modified Garcia test, forelimb placement test, and corner turn test at 24 h after ICH. The neurofunctional improvements seen with rCTRP9 therapy were reversed by administration of AdipoR1 siRNA and specific PI3 K inhibitor LY294002 (p<0.05 compared with ICH+rCTRP9, Fig. 5A-C).

rCTRP9 Attenuated Neuronal Apoptosis Through AdipoR1/PI3K/Akt Signaling after ICH

Administration of rCTRP9 resulted in significantly greater protein expressions of AdipoR1 and PI3 K within the affected brain hemispheres of treated ICH animals when compared with the sham and ICH+vehicle groups at 24 h

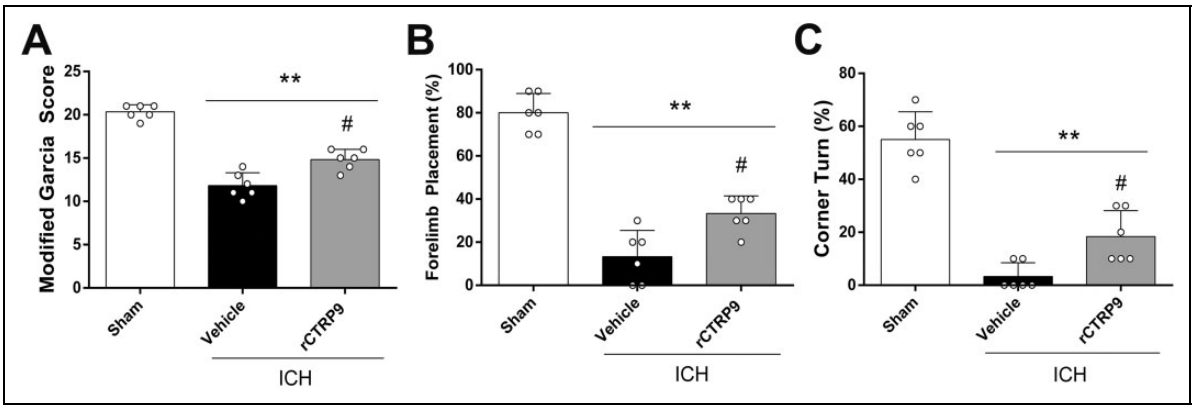

Figure 2. The effects of rCTRP9 on short-term neurobehavioral function at 24 h after ICH. (A) Modified Garcia test, (B) Forelimb placement test, and (C) Corner turn test at 24 h post-ICH. Values are expressed as mean ± SD. $^{**}p<0.01$ vs. sham group; $^{\#}p<0.05$ vs. vehicle group; $N=6$.

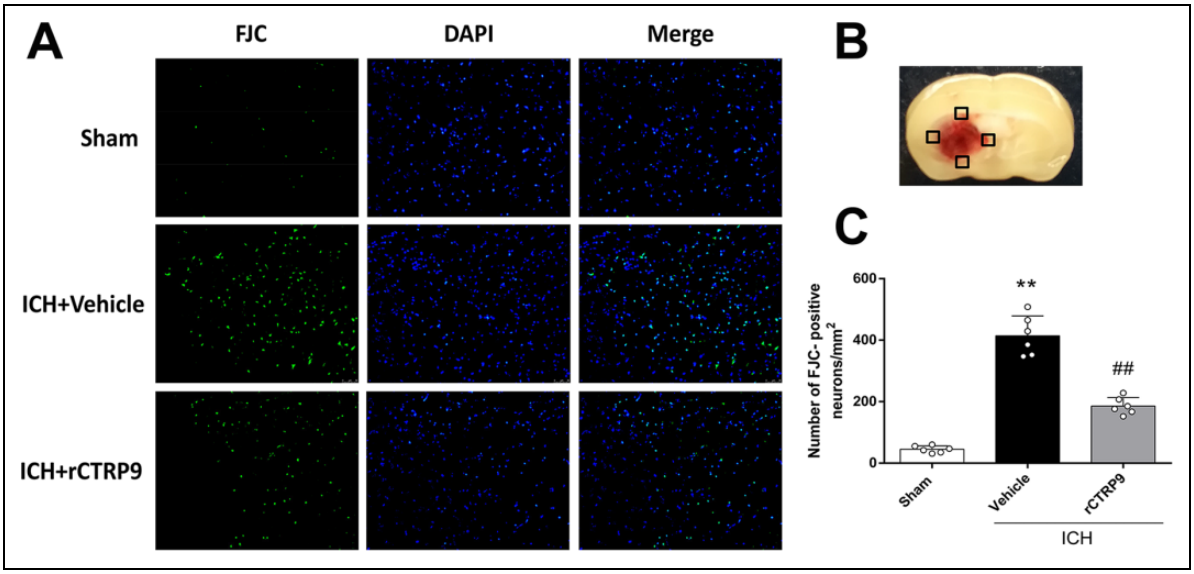

Figure 3. The effects of rCTRP9 on neuronal degenerating at 24 h after ICH. (A) Representative microphotographs of Fluoro-Jade C staining (FJC)-positive neurons. (B) Quantitative analysis of FJC-positive cells was performed at the ipsilateral cortex. (C) FJC-positive neurons significantly increased after ICH induction. Vehicle, phosphate-buffered saline (PBS); rCTRP9, 0.1 μg/g of rCTRP9 treated 1 h after ICH induction. $^{**}p< 0.01$ vs. sham group; $^{\#\#}p< 0.01$ vs. ICH+vehicle group. Values are expressed as mean ± SD. $N=3$.

after surgery ($p<0.05$, Fig. 6A, B). Moreover, the expressions of phosphorylated Akt, Bcl-2 were significantly increased, while the expression of Bax was significantly decreased in the ICH+rCTRP9 group when compared with the ICH+vehicle group at 24 h after surgery ($p<0.05$, Fig. 6A, B). However, inhibition of AdipoR1 with AdipoR1 siRNA significantly decreased the expression of AdipoR1, PI3 K, phosphorylated Akt and Bcl-2, and increased the expression of Bax when compared with the ICH+rCTRP9+scr siRNA group at 24 h after ICH ($p<0.05$, Fig. 6B). Similarly, pretreatment with LY294002 significantly decreased the expression of PI3 K and the expression of the downstream molecules p-Akt, as well as Bcl-2 and increased the expression of Bax in the ICH+rCTRP9+LY294002 group when compared with the ICH+rCTRP9+DMSO group at 24 h after ICH ($p<0.05$, Fig. 6B).

Discussion

In this present study, we first investigated the potential anti-apoptosis effect of rCTRP9 and explored the possible underlying mechanism of rCTRP9 after ICH. We discovered that the expression of AdipoR1 and rCTRP9 increased after ICH induction. AdipoR1 was found to be expressed in neurons, astrocytes, and microglia cells. Administration of rCTRP9 attenuated neuronal apoptosis and preserved neurological

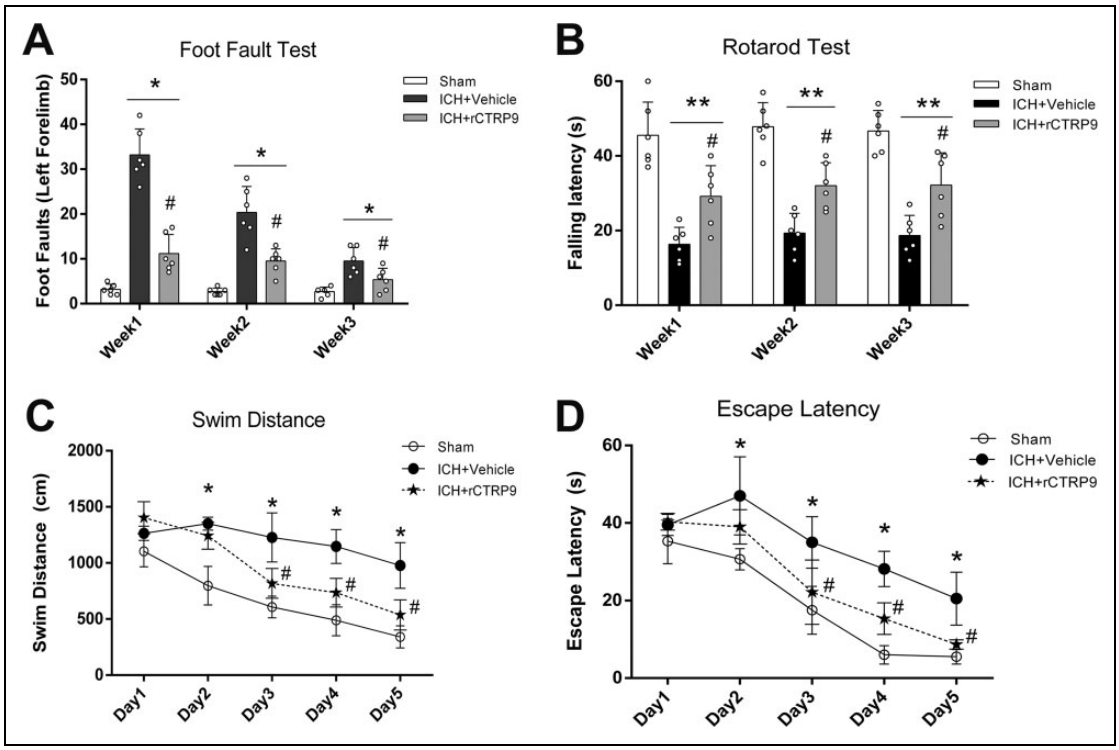

Figure 4. The effects of rCTRP9 on the long-term neurobehavioral function after ICH. (A) Foot-fault test in the first, second, and third week after ICH. (B) Rotarod test in the first, second, and third week after ICH. (C) Swim distance of Morris water maze on days 21 to 25 after ICH. (D) Escape latency of Morris water maze results on days 21–25 after ICH. Values are expressed as mean ± SD. *p<0.05 vs. sham group; #p<0.05 vs. ICH+vehicle group. N=8.

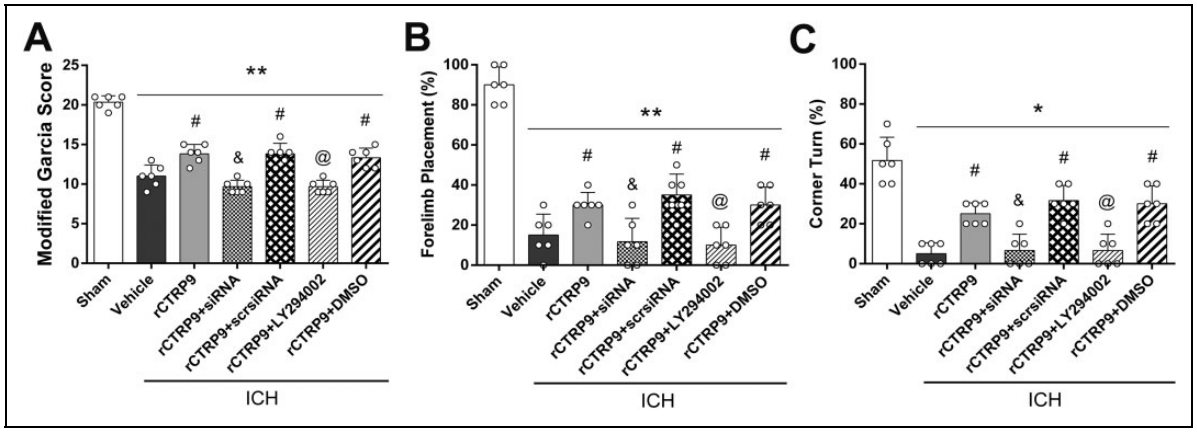

Figure 5. Knockdown of AdipoR1 and inhibition of PI3 K abolished improvement in neurological function of rCTRP9 at 24 h after ICH. (A) Modified Garcia test. (B) Forelimb placement test. (C) Corner turn test. Values are expressed as mean ± SD. *p<0.05, **p<0.01 vs. sham group; #p<0.05 vs. vehicle group; and p<0.05 vs. rCTRP9+Scr siRNA, and @p<0.05 vs. rCTRP9+DMSO group. Scr, scramble; and siRNA, small interfering RNA. N=6.

function after ICH. Administration of rCTRP9 was associated with upregulation of AdipoR1, PI3 K, p-Akt, and Bcl-2, and downregulation of Bax after ICH. However, blockage of AdipoR1 and PI3 K reversed the beneficial effects of rCTRP9 on neurofunctional deficits and neuronal apoptosis. Conclusively, our findings suggest that administration of rCTRP9 might attenuate neuronal apoptosis after ICH, which was, at least in part, mediated by the AdipoR1/PI3K/Akt signaling pathway.

The APN receptor is an emerging potential target in diverse CNS disease[36–38]. Activation of APN receptors results in adequate regulation of cellular metabolism, and

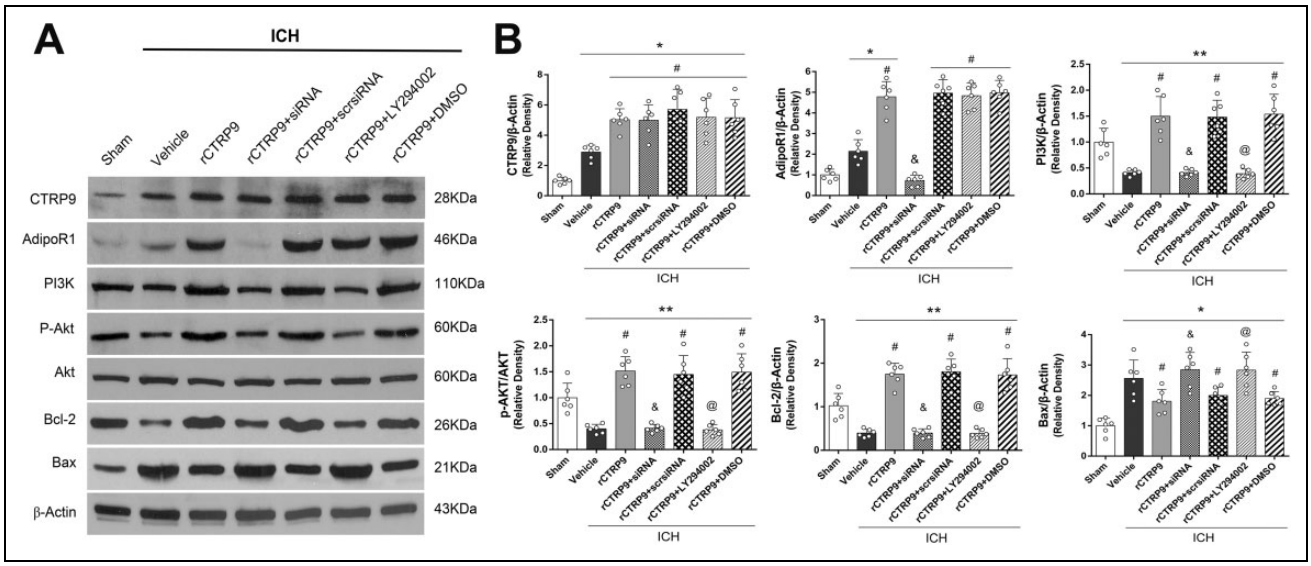

Figure 6. Knockdown of AdipoR1 and inhibition of PI3 K reversed the effects of rCTRP9 after ICH. (A) Representative western blot images. (B) Quantitative analyses of CTRP9, AdipoR1, PI3 K, p-Akt/Akt, Bcl-2 and Bax at 24 h post-ICH. Values are expressed as mean ± SD. *$p<0.05$, **$p<0.01$ vs. sham group; $^{\#}p<0.05$ vs. vehicle group; $^{\&}p<0.05$ vs. rCTRP9+Scr siRNA, and $^{@}p<0.05$ vs. rCTRP9+DMSO group. $N=6$.

exerts anti-atherosclerosis and anti-inflammatory effects[39–41]. Although APN receptors have been shown to exist abundantly in the brain, their exact role in brain diseases remains unclear. Two APN receptors have been identified: AdipoR1 and AdipoR2. Recent studies reported that AdipoR1 and AdipoR2 are both expressed within cortical neurons of mice, with AdipoR1 being more pronounced than AdipoR2[42]. Furthermore, AdipoR1 binds to globular APN with higher affinity than AdipoR2. AdipoR2 has an intermediate binding affinity for both globular APN and full-length APN[17]. Previous studies revealed that AdipoR1 was widely expressed in neurons, astrocytes, and microglial cells[43]. Furthermore, our results indicate that the expression of AdipoR1 increases within 24 h following ICH. Based on our immunohistochemistry data, the expression of AdipoR1 was observed in neurons, astrocytes, and microglia, which is consistent with the results of the aforementioned studies. The increase in AdipoR1 expression within the ipsilateral brain hemisphere after ICH inductions requires further explanation; however, we suggest that the observed change in AdipoR1 expression might be a response to the stress reaction induced by ICH. Moreover, the expression of AdipoR1 was further elevated after administration of rCTRP9. The effects of rCTRP9 on AdipoR1 expression were consistent with the results of a previous study, which showed that APN increased the expression of AdipoR1 and protected the brain tissue against the detrimental effects of ischemic stroke[44].

APN is an adipokine that is predominantly secreted by adipocytes. It has numerous functions, including regulation of metabolism, anti-inflammation, protection against endothelial dysfunction, and protection against ischemic injury[40,41]. The CTRPs are a newly discovered, highly conserved family of APN paralogs, containing 15 members (CTRP1 to CTRP15). This specific protein family exhibits similar structure as APN, consisting of four distinct domains including a N-terminal signal peptide, a short variable domain, a collagen-like domain, and a C-terminal C1q-like globular domain[45,46]. Of all CTRP paralogs, CTRP9 shows the highest degree of amino acid identity to APN in its globular C1q domain. In the present study, we demonstrated for the first time that CTRP9 has anti-apoptotic effects protecting neurons from ICH-induced SBI. Furthermore, we evaluated the temporal expression of endogenous CTRP9 within 72 h after experimental ICH. The results indicated that CTRP9 expression increased after ICH and reached the highest level at 24 h from ICH induction.

It is generally believed that neuronal apoptosis is a crucial process leading to secondary neurological damage after ICH[47,48]. The anti-apoptotic effects of AdipoR1 have been reported in an obese model[44]. It has been reported that APN receptor activation attenuates human hepatocytes, HepG2 cells apoptosis via the PI3K/Akt pathway[49]. Two recent studies suggest that the anti-apoptotic effects of AdipoR1 agonists are mediated via PI3K/Akt signaling pathway[50].

Although anti-apoptotic effects of APN have been previously reported in many disease models[51–53], the underlying mechanism remains unclear. PI3 K is a protein tyrosine kinase activated by a cytokine receptor. Activated PI3 K activates cytoplasmic Akt via phosphorylation, thereby regulating expression of genes involved in cell survival, proliferation, cell-cycle progression, and angiogenesis in cerebral development and disorders[54,55]. It has been reported that activated PI3K/Akt signaling improves neurological function and attenuates neuronal apoptosis in murine models of

subarachnoid hemorrhage (SAH)[34]. The present study showed that CTRP9 treatment attenuated neuronal apoptosis following ICH. Specifically, CTRP9 treatment upregulated the expression of the targeted proteins on the pathway (AdipoR1, PI3 K, and p-Akt) as well as the anti-apoptotic molecular marker (Bcl-2) and downregulated the expression of the pro-apoptotic molecular marker (Bax). When AdipoR1 was silenced by AdipoR1 siRNA pretreatment, expression of AdipoR1, PI3 K, p-Akt, Bcl-2 was suppressed and expression of Bax was enhanced, suggesting that anti-apoptotic effects of CTRP9 were abolished. Similarly, pretreatment with a PI3 K inhibitor blocked the activation of PI3 K and p-Akt by rCTRP9, leading to decreased expression of anti-apoptotic marker (Bcl-2) and increased expression of pro-apoptotic marker (Bax). These findings suggest that activation of PI3K/Akt signaling pathway underlies the anti-apoptotic effects of CTRP9.

There were some limitations in our study. First, the present study did not rule out the possible neuroprotective effects of CTRP9 through preservation of the blood–brain barrier or alleviation of neuroinflammation. Therefore, further studies must be conducted to explore the aforementioned possibilities. Second, the pathophysiology of neuronal apoptosis after ICH is a complex network. Other downstream factors such as mitogen-activated protein kinase (MAPK), adenosine monophosphate-activated protein kinase (AMPK) may be modulated by rCTRP9 administration after ICH, which was not explored in this study. Another limitation is that we have evaluated the total expression of PI3 K rather than its activated phosphorylated form.

In the current study, we focused on AdipoR1/PI3K/Akt signaling in regards to anti-apoptotic molecular mechanisms. Further studies need to be conducted to explore other potential signaling pathways contributed by rCTRP9 and AdipoR1 activation. Third, in our experiments, we used adult CD1 mice to mimic the progression of ICH; however, ICH tends to occur in older patients with hypertension, vascular disorders, and cerebral amyloid angiopathy[56]. We did not evaluate the effects of rCTRP9 in different age groups or in animals with systemic co-morbidities.

Conclusions

In summary, we showed for the first time that rCTRP9 administration improved neurological function and reduced neuronal apoptosis through AdipoR1/PI3K/Akt pathway in an experimental ICH model. Therefore, administration of rCTRP9 may be a promising therapeutic strategy in ICH management. Further studies need to evaluate further mechanisms and applications of rCTRP9 in the CNS.

Authors' Contributions

JHZ, LHZ, and JPT conceived and designed the study. LHZ, SPC, JPT and PS performed the experiments and collected the data. LHZ, PS, WZ, PK, and JHZ contributed to analyzing the data and drafting this article. All authors read and approved the final manuscript.

Ethical Approval

All animal experiments in this study were performed with approval of the Institutional Animal Care and Use Committee (IACUC) at Loma Linda University (IACUC No. 8160049).

Statement of Human and Animal Rights

All procedures in this study followed the Health's Guide for the Care and Use of Laboratory Animals (National Research Council) and complied with the ARRIVE (Animal Research: Reporting of In Vivo Experiments) guidelines for reporting in vivo experiments.

Statement of Informed Consent

There are no human subjects in this article and informed consent is not applicable.

Declaration of Conflicting Interests

The authors declared no potential conflicts of interest with respect to the research, authorship, and/or publication of this article.

Funding

The authors disclosed receipt of the following financial support for the research, authorship, and/or publication of this article: This study is supported partially by grants from National Institutes of Health (NS091042 and NS082184) to Dr. J. H. Zhang.

Supplemental Material

Supplemental material for this article is available online.

References

1. Steiner T, Al-Shahi Salman R, Beer R, et al. European Stroke Organisation (eso) guidelines for the management of spontaneous intracerebral hemorrhage. Int J Stroke. 2014;9(7):840–855.
2. Rodriguez-Yanez M, Castellanos M, Freijo MM, et al. Clinical practice guidelines in intracerebral haemorrhage. Neurologia. 2013;28(4):236–249.
3. Xi G, Strahle J, Hua Y, Keep RF. Progress in translational research on intracerebral hemorrhage: is there an end in sight? Prog Neurobiol. 2014;115:45–63.
4. Dixit D, Thomas Z. Letter by Dixit and Thomas regarding article, "guidelines for the management of spontaneous intracerebral hemorrhage: a guideline for healthcare professionals from the American Heart Association/American Stroke Association". Stroke. 2015;46(11):e236.
5. Matsushita K, Meng W, Wang X, Asahi M, Asahi K, Moskowitz MA, Lo EH. Evidence for apoptosis after intercerebral hemorrhage in rat striatum. J Cereb Blood Flow Metab. 2000;20(2):396–404.
6. Qureshi AI, Suri MF, Ostrow PT, Kim SH, Ali Z, Shatla AA, Guterman LR, Hopkins LN. Apoptosis as a form of cell death in intracerebral hemorrhage. Neurosurgery. 2003;52(5):1041–1047; discussion 1047–1048.
7. Yang D, Han Y, Zhang J, Ding C, Anagli J, Seyfried DM. Improvement in recovery after experimental intracerebral hemorrhage using a selective cathepsin B and l inhibitor. J Neurosurg. 2011;114(4):1110–1116.

8. Pang J, Peng J, Matei N, Yang P, Kuai L, Wu Y, Chen L, Vitek MP, Li F, Sun X, Zhang JH, Jiang Y. Apolipoprotein E exerts a whole-brain protective property by promoting M1? Microglia quiescence after experimental subarachnoid hemorrhage in mice. Transl Stroke Res. 2018;9(6):654–668.
9. Kuwashiro T, Ago T, Kamouchi M, Matsuo R, Hata J, Kuroda J, Fukuda K, Sugimori H, Fukuhara M, Awano H, Isomura T, Suzuki K, Yasaka M, Okada Y, Kiyohara Y, Kitazono T. Significance of plasma adiponectin for diagnosis, neurological severity and functional outcome in ischemic stroke - research for biomarkers in ischemic stroke (REBIOS). Metabolism. 2014;63(9):1093–1103.
10. Kadowaki T, Yamauchi T, Kubota N, Hara K, Ueki K, Tobe K. Adiponectin and adiponectin receptors in insulin resistance, diabetes, and the metabolic syndrome. J Clin Invest. 2006; 116(7):1784–1792.
11. Turer AT, Scherer PE. Adiponectin: mechanistic insights and clinical implications. Diabetologia. 2012;55(9):2319–2326.
12. Ma K, Cabrero A, Saha PK, Kojima H, Li L, Chang BH, Paul A, Chan L. Increased beta-oxidation but no insulin resistance or glucose intolerance in mice lacking adiponectin. J Biol Chem. 2002;277(38):34658–34661.
13. Kishore U, Gaboriaud C, Waters P, Shrive AK, Greenhough TJ, Reid KB, Sim RB, Arlaud GJ. C1q and tumor necrosis factor superfamily: modularity and versatility. Trends Immunol. 2004;25(10):551–561.
14. Wong GW, Krawczyk SA, Kitidis-Mitrokostas C, Revett T, Gimeno R, Lodish HF. Molecular, biochemical and functional characterizations of c1q/TNF family members: adipose-tissue-selective expression patterns, regulation by PPAR-gamma agonist, cysteine-mediated oligomerizations, combinatorial associations and metabolic functions. Biochem J. 2008; 416(2):161–177.
15. Wong GW, Krawczyk SA, Kitidis-Mitrokostas C, Ge G, Spooner E, Hug C, Gimeno R, Lodish HF. Identification and characterization of CTRP9, a novel secreted glycoprotein, from adipose tissue that reduces serum glucose in mice and forms heterotrimers with adiponectin. FASEB J. 2009;23(1): 241–258.
16. Davis KE, Scherer PE. Adiponectin: no longer the lone soul in the fight against insulin resistance? Biochem J. 2008;416(2): e7–e9.
17. Thundyil J, Pavlovski D, Sobey CG, Arumugam TV. Adiponectin receptor signalling in the brain. Br J Pharmacol. 2012; 165(2):313–327.
18. Xu N, Zhang Y, Doycheva DM, Ding Y, Zhang Y, Tang J, Guo H, Zhang JH. Adiponectin attenuates neuronal apoptosis induced by hypoxia-ischemia via the activation of AdipoR1/APPL1/LKB1/AMPK pathway in neonatal rats. Neuropharmacology. 2018;133:415–428.
19. Liu J, Sui H, Zhao J, Wang Y. Osmotin protects H9c2 cells from simulated ischemia-reperfusion injury through AdipoR1/PI3K/AKT signaling pathway. Front Physiol. 2017;8:611.
20. Wijesekara N, Krishnamurthy M, Bhattacharjee A, Suhail A, Sweeney G, Wheeler MB. Adiponectin-induced ERK and AKT phosphorylation protects against pancreatic beta cell apoptosis and increases insulin gene expression and secretion. J Biol Chem. 2010;285(44):33623–33631.
21. Kambara T, Shibata R, Ohashi K, Matsuo K, Hiramatsu-Ito M, Enomoto T, Yuasa D, Ito M, Hayakawa S, Ogawa H, Aprahamian T, Walsh K, Murohara T, Ouchi N. C1q/tumor necrosis factor-related protein 9 protects against acute myocardial injury through an adiponectin receptor I-AMPK-dependent mechanism. Mol Cell Biol. 2015;35(12):2173–2185.
22. Li Q, Zhu Z, Wang C, Cai L, Lu J, Wang Y, Xu J, Su Z, Zheng W, Chen X. Ctrp9 ameliorates cellular senescence via PGC1alpha/AMPK signaling in mesenchymal stem cells. Int J Mol Med. 2018;42(2):1054–1063.
23. Manaenko A, Yang P, Nowrangi D, Budbazar E, Hartman RE, Obenaus A, Pearce WJ, Zhang JH, Tang J. Inhibition of stress fiber formation preserves blood-brain barrier after intracerebral hemorrhage in mice. J Cereb Blood Flow Metab. 2018;38(1): 87–102.
24. Endo H, Nito C, Kamada H, Yu F, Chan PH. Akt/GSK3beta survival signaling is involved in acute brain injury after subarachnoid hemorrhage in rats. Stroke. 2006;37(8):2140–2146.
25. Salahpour A, Medvedev IO, Beaulieu JM, Gainetdinov RR, Caron MG. Local knockdown of genes in the brain using small interfering RNA: a phenotypic comparison with knockout animals. Biol Psychiatry. 2007;61(1):65–69.
26. Yang P, Wu J, Miao L, Manaenko A, Matei N, Zhang Y, Xu L, Pearce WJ, Hartman RE, Obenaus A, Zhang JH, Xu F, Tang J. Platelet-derived growth factor receptor-beta regulates vascular smooth muscle cell phenotypic transformation and neuroinflammation after intracerebral hemorrhage in mice. Crit Care Med. 2016;44(6):e390–e402.
27. Zhang Y, Chen Y, Wu J, Manaenko A, Yang P, Tang J, Fu W, Zhang JH. Activation of dopamine d2 receptor suppresses neuroinflammation through alphaB-crystalline by inhibition of NF-kappaB nuclear translocation in experimental ICH mice model. Stroke. 2015;46(9):2637–2646.
28. Chen Y, Zhang Y, Tang J, Liu F, Hu Q, Luo C, Tang J, Feng H, Zhang JH. Norrin protected blood-brain barrier via frizzled-4/beta-catenin pathway after subarachnoid hemorrhage in rats. Stroke. 2015;46:529–536.
29. Hua Y, Schallert T, Keep RF, Wu J, Hoff JT, Xi G. Behavioral tests after intracerebral hemorrhage in the rat. Stroke. 2002; 33(10):2478–2484.
30. Tong LS, Shao AW, Ou YB, Guo ZN, Manaenko A, Dixon BJ, Tang J, Lou M, Zhang JH. Recombinant Gas6 augments Axl and facilitates immune restoration in an intracerebral hemorrhage mouse model. J Cereb Blood Flow Metabo. 2017;37(6): 1971–1981.
31. Li Z, Wang J, Zhao C, Ren K, Xia Z, Yu H, Jiang K. Acute blockage of notch signaling by DAPT induces neuroprotection and neurogenesis in the neonatal rat brain after stroke. Transl Stroke Res. 2016;7(2):132–140.
32. Xie Z, Huang L, Enkhjargal B, Reis C, Wan W, Tang J, Cheng Y, Zhang JH. Intranasal administration of recombinant netrin-1 attenuates neuronal apoptosis by activating DCC/APPL-1/AKT signaling pathway after subarachnoid hemorrhage in rats. Neuropharmacology. 2017;119:123–133.

33. Lekic T, Hartman R, Rojas H, Manaenko A, Chen W, Ayer R, Tang J, Zhang JH. Protective effect of melatonin upon neuropathology, striatal function, and memory ability after intracerebral hemorrhage in rats. J Neurotrauma. 2010;27(3):627–637.
34. Xie Z, Enkhjargal B, Wu L, Zhou K, Sun C, Hu X, Gospodarev V, Tang J, You C, Zhang JH. Exendin-4 attenuates neuronal death via GLP-1R/PI3k/Akt pathway in early brain injury after subarachnoid hemorrhage in rats. Neuropharmacology. 2018; 128:142–151.
35. Yu L, Lu Z, Burchell S, Nowrangi D, Manaenko A, Li X, Xu Y, Xu N, Tang J, Dai H, Zhang JH. Adropin preserves the blood-brain barrier through a Notch1/Hes1 pathway after intracerebral hemorrhage in mice. J Neurochem. 2017;143(6): 750–760.
36. Song J, Choi SM, Whitcomb DJ, Kim BC. Adiponectin controls the apoptosis and the expression of tight junction proteins in brain endothelial cells through AdipoR1 under beta amyloid toxicity. Cell Death Disease. 2017;8(10):e3102.
37. Zhang D, Wang X, Wang B, Garza JC, Fang X, Wang J, Scherer PE, Brenner R, Zhang W, Lu XY. Adiponectin regulates contextual fear extinction and intrinsic excitability of dentate gyrus granule neurons through AdipoR2 receptors. Mol Psychiatry. 2017;22(7):1044–1055.
38. Yue L, Zhao L, Liu H, Li X, Wang B, Guo H, Gao L, Feng D, Qu Y. Adiponectin protects against glutamate-induced excitotoxicity via activating SIRT1-dependent PGC-1alpha expression in HT22 hippocampal neurons. Oxid Med Cell Longev. 2016;2016:2957354.
39. Okamoto Y, Kihara S, Ouchi N, Nishida M, Arita Y, Kumada M, Ohashi K, Sakai N, Shimomura I, Kobayashi H, Terasaka N, Inaba T, Funahashi T, Matsuzawa Y. Adiponectin reduces atherosclerosis in apolipoprotein E-deficient mice. Circulation. 2002;106(22):2767–2770.
40. Lara-Castro C, Fu Y, Chung BH, Garvey WT. Adiponectin and the metabolic syndrome: mechanisms mediating risk for metabolic and cardiovascular disease. Curr Opin Lipidol. 2007; 18(3):263–270.
41. Kang KH, Higashino A, Kim HS, Lee YT, Kageyama T. Molecular cloning, gene expression, and tissue distribution of adiponectin and its receptors in the Japanese monkey, Macaca fuscata. J Med Primatol. 2009;38(2):77–85.
42. Guillod-Maximin E, Roy AF, Vacher CM, Aubourg A, Bailleux V, Lorsignol A, Penicaud L, Parquet M, Taouis M. Adiponectin receptors are expressed in hypothalamus and colocalized with proopiomelanocortin and neuropeptide y in rodent arcuate neurons. J Endocrinol. 2009;200(1):93–105.
43. Kadowaki T, Yamauchi T. Adiponectin and adiponectin receptors. Endocrine Rev. 2005;26:439–451.
44. Guo F, Jiang T, Song W, Wei H, Wang F, Liu L, Ma L, Yin H, Wang Q, Xiong L. Electroacupuncture attenuates cerebral ischemia-reperfusion injury in diabetic mice through adiponectin receptor 1-mediated phosphorylation of GSK-3beta. Mol Neurobiol. 2015;51(12):685–695.
45. Wong GW, Wang J, Hug C, Tsao TS, Lodish HF. A family of ACRP30/adiponectin structural and functional paralogs. Proc Natl Acad Sci U S A. 2004;101(28):10302–10307.
46. Wei Z, Peterson JM, Wong GW. Metabolic regulation by c1q/TNF-related protein-13 (CTRP13): activation of amp-activated protein kinase and suppression of fatty acid-induced JNK signaling. J Biol Chem. 2011;286(18):15652–15665.
47. Egawa N, Lok J, Washida K, Arai K. Mechanisms of axonal damage and repair after central nervous system injury. Transl Stroke Res. 2017;8(1):14–21.
48. Xiong XY, Yang QW. Rethinking the roles of inflammation in the intracerebral hemorrhage. Transl Stroke Res. 2015;6(5): 339–341.
49. Chou IP, Lin YY, Ding ST, Chen CY. Adiponectin receptor 1 enhances fatty acid metabolism and cell survival in palmitate-treated HepG2 cells through the PI3K/AKT pathway. Eur J Nutr. 2014;53:907–917.
50. Shah SA, Lee HY, Bressan RA, Yun DJ, Kim MO. Novel osmotin attenuates glutamate-induced synaptic dysfunction and neurodegeneration via the JNK/PI3K/AKT pathway in postnatal rat brain. Cell Death Disease. 2014;5:e1026.
51. Ohashi K, Shibata R, Murohara T, Ouchi N. Role of anti-inflammatory adipokines in obesity-related diseases. Trends Endocrinol Metab. 2014;25(7):348–355.
52. Yang Y, Hu W, Jiang S, Wang B, Li Y, Fan C, Di S, Ma Z, Lau WB, Qu Y. The emerging role of adiponectin in cerebrovascular and neurodegenerative diseases. Biochim Biophys Acta. 2015;1852(9):1887–1894.
53. Wang Y, Zhou M, Lam KS, Xu A. Protective roles of adiponectin in obesity-related fatty liver diseases: mechanisms and therapeutic implications. Arq Bras Endocrinol Metabol. 2009; 53(2):201–212.
54. Gao X, Zhang H, Steinberg G, Zhao H. The AKT pathway is involved in rapid ischemic tolerance in focal ischemia in rats. Transl Stroke Res. 2010;1(3):202–209.
55. Wang B, Guo H, Li X, Yue L, Liu H, Zhao L, Bai H, Liu X, Wu X, Qu Y. Adiponectin attenuates oxygen-glucose deprivation-induced mitochondrial oxidative injury and apoptosis in hippocampal HT22 cells via the JAK2/STAT3 pathway. Cell Transplant. 2018;1:963689718779364.
56. Xie Y, Li YJ, Lei B, Kernagis D, Liu WW, Bennett ER, Venkatraman T, Lascola CD, Laskowitz DT, Warner DS, James ML. Sex differences in gene and protein expression after intracerebral hemorrhage in mice. Transl Stroke Res. 2019;10(2):231–239.